Proceedings of the International Symposium on Physics of Materials (ISPMA13)

Tool Steels: Forging Simulation and Microstructure Evolution of Large Scale Ingot

S. Mengaroni[a,*], F. Cianetti[a], M. Calderini[b], E. Evangelista[b], A. Di Schino[c] and H. McQueen[d]

[a]Università degli Studi di Perugia, Via G. Duranti 63, I06125 Perugia, Italy
[b]Società delle Fucine, Viale B. Brin 218, I05100 Terni, Italy
[c]Centro Sviluppo Materiali S.p.A., Via di Castel Romano 100, I00128 Roma, Italy
[d]Concordia University, 1455 Maisonneuve W. EV 3.420, Montreal, H3G 1M8, Canada

The aim of this paper is to analyze the hot working behavior of two different steels based on 3% and 5% Cr steel chemistry, respectively. Hot deformation is studied by hot torsion tests in the range of temperatures 1000–1200 °C and strain rates 0.01, 0.10, 1.00 s^{-1}. At given temperatures and strain rates flow curves exhibit a peak followed by a decline towards a steady state which is indicative of dynamic recrystallization. At constant strain, flow stress increases with increasing strain rate and decreasing temperature. The analysis of the constitutive equation relating peak flow stress, strain rate and temperature shows high activation energy values for both steels. Recrystallized volume fraction of steels after hot deformation is estimated based on the grain orientation spread as measured by electron backscattered diffraction technique, on the hot deformed and quenched materials.

DOI: 10.12693/APhysPolA.128.629
PACS: 06.60.Ei, 61.05.J–, 81.05.Bx

1. Introduction

It is well known that the hot work processing of steels is mainly influenced by strain rate ($\dot{\varepsilon}$) and temperature (T) and that the optimization of them allows the steels under forming to recrystallize dynamically to fine grains without cracks [1–4].

A way to study the hot deformation process in steels is hot torsion test [1, 2, 5, 6]. Hot-torsion test consists of twisting a cylindrical specimen at a defined rate to a certain strain or to failure and it provides information on the hot deformation under defined conditions of temperature and strain rates. The hot deformation mechanisms are involved when temperature is above $0.5T_m$ (melting temperature, K) and the phenomena are similar to creep [1–7].

The goal is to find the constitutive equations of steels so to define the relationship between stress, strain, strain rate and temperature based on the study of the shape of the stress–strain curve; that is influenced by work hardening, dynamic recovery and/or dynamic recrystallization. Dynamic recrystallization (DRX), is one of the main softening mechanisms at high temperature, nucleation takes place at approximately 0.3–4 of ε_{p} where softening equals hardening.

The flow curves can be divided into three successive stages: during the first stage, work hardening and dynamic recovery occur at relatively low strains. This stage is characterized by the increase in dislocation density, the elongation of grains by forming the so-called "pancake" microstructure and the formation of subgrains within the deformed grains. At large strains, a steady state regime is reached and the final microstructure becomes equiaxed; a transition zone characterized by a drop in the true stress, attributed to the occurrence of dynamic recrystallization. The decrease in stress can take place in different ways: single peak behavior observed at low temperatures and high strain rates, and multiple peaks at high temperatures and/or low strain rates; a stabilization of the stress–strain curve up to the failure of the sample.

For the peak a power law is often found [8, 9]:

$$\dot{\varepsilon} = A_0 \exp\left(\frac{-Q}{RT}\right)\sigma^n, \tag{1}$$

where A_0, Q, R (gas constant) and n can be considered constants.

If the Zener–Hollomon parameter is defined as [3]:

$$Z = \dot{\varepsilon}\exp\left(\frac{-Q}{RT}\right), \tag{2}$$

the following power law is obtained [1]:

$$Z = A_0\sigma^n. \tag{3}$$

Garofalo extended the above approach proposing an expression that covered the whole range of stresses [2]:

$$\dot{\varepsilon} = A'\exp\left(\frac{-Q}{RT}\right)[\sinh(\alpha\sigma)]^{n'}, \tag{4}$$

where A', n', Q, R and α are constants.

Steels based on 3% and 5% Cr respectively are used for the production of heavy components, usually forged in 3 or 4 steps and the forging process involves high costs.

The aim of this work is to study the hot deformation behavior in order to optimize the forging process. The steels are usually used in the quenched and tempered state, characterized by tempered martensitic microstructure.

*corresponding author; e-mail: sabrinamengaroni@gmail.com

2. Material and experimental details

Steel 1 and 2 are considered in this study, the first being a 3% Cr, the second a 5% Cr steel (Table I).

TABLE I

Steels chemical composition (wt%).

	C	Mo	Cr	V
steel 1	0.40	0.65	3.30	0.12
steel 2	0.45	0.50	5.30	0.16

Specimens of both steels have undergone torsion tests at 1000, 1100, 1200 °C, and true strain rate at specimen surface of 0.01, 0.10, 1.00 s^{-1}, in controlled Ar atmosphere. In order to simulate the forging process, specimens of steels 1 and 2 were heated by a high frequency induction coil (1 °C/s) up to 1200 °C (temperature of industrial forging); the deformation process was carried out in 5 min: after deformation the specimen was hold at constant temperature (the same temperature at which deformation was carried out) for 5 s and then rapidly water quenched to room temperature. A thermocouple was inserted inside the specimen to control temperature during the tests. A computer program acquired the torque (M) versus twist angle (θ) data. The $M-\theta$ data generally give no useful information about the material, unless the geometry of specimen is specified. It is usually customary to convert the torque, the angle of twist and angular velocity to equivalent stress, strain and strain rate, respectively.

By hot torsion tests n coefficient in (1) and n' in (4) have been evaluated plotting stress and strain rate in a logarithmic plane. The activation energy Q is determined plotting in a semilogarithmic plane the stress versus the inverse of the temperature. The coefficient A_0 for (1) and A' for (4) are reached in a logarithmic plot of Z versus stress.

The specimen microstructure was investigated by means of transmission electron microscopy (TEM) and orientation image microscopy (OIM) techniques using electron backscattered diffraction (EBSD) pattern. By this technique, the surface of a crystalline material with low dislocation density can be scanned and in each point the orientation of the underlying grain can be determined in a fully automatic way. From these measurements some microstructural characteristics of the material can be estimated, e.g. misorientations between adjacent grains, crystallographic orientations, etc. It is of great importance to assess the grain size, because this parameter greatly influences the strength and the cleavage fracture resistance of ferritic steels. EBSD is a very accurate method to measure the effective grain size, even for fine microstructures. By means of this technique it is possible to evaluate the recrystallized area fraction based on parameter considering the grain misorientation. In particular the grain orientation spread (GOS) parameter points out the average deviation between the orientation of each point in the grain and the average orientation of the grain. The recrystallized grains are resolved from the EBSD maps by applying a criterion that the GOS value must be smaller than 1 degree [10–12].

3. Results and discussion

3.1. Constitutive equations

The flow stress–strain curves for steel 1 are reported in Fig. 1. Both peak flow stresses and strains are shown for different strain rates and temperatures. The peak followed by flow softening that decreases with rising temperature reveals that dynamic recrystallization occurs.

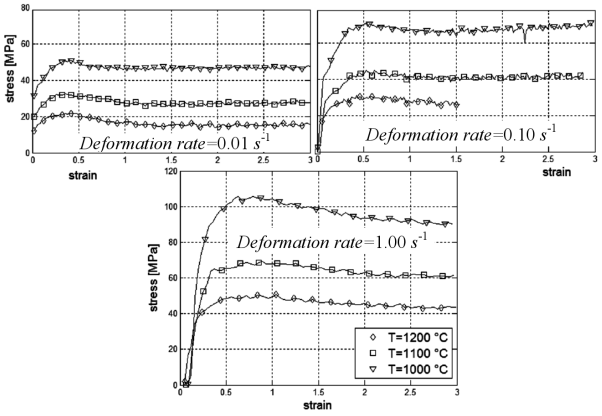

Fig. 1. Steel 1 flow stress–strain curve.

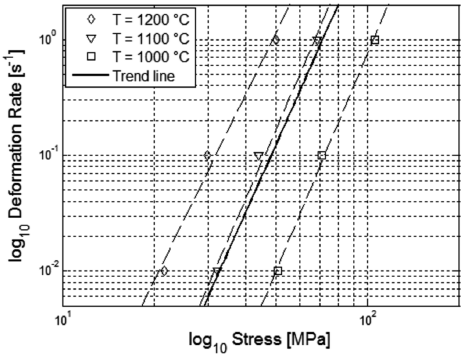

Fig. 2. Steel 1 definition of n' coefficient.

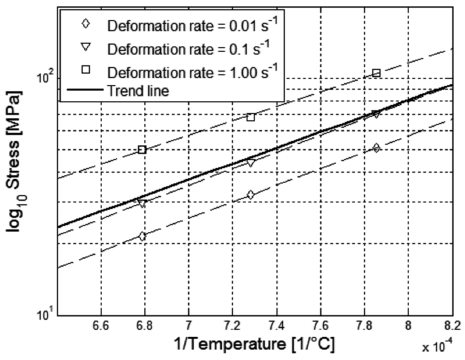

Fig. 3. Steel 1 definition of Q coefficient.

The n' coefficient has been evaluated in a logarithmic plot, stress and strain rate (Fig. 2) while the activation energy Q is determined plotting in a semilogarithmic plane the stress versus the inverse of the temperature (Fig. 3). Both coefficients are relative to steel 1.

TABLE II

Constitutive coefficients for Eq. (1).

	Steel 1	Steel 2
n	5.91	7.10
Q [kJ mol^{-1}]	378	440
A_0	3946.60	8037.40

TABLE III

Constitutive coefficients for Eq. (4)

	Steel 1	Steel 2
n'	5.78	5.70
Q [kJ mol^{-1}]	376	415
A'	3.28×10^{17}	3.28×10^{15}
A	0.004	0.013

Table II shows the value of constants of both steels using Eq. (1) while Table III shows the constants value of both steels using Eq. (4).

The comparison between experimental stress and calculated one shows that they are similar using Eqs. (1) and (4) for both steels (Fig. 4) From such results a similar hot deformation behavior is found for steels 1 and 2, independently of Cr content.

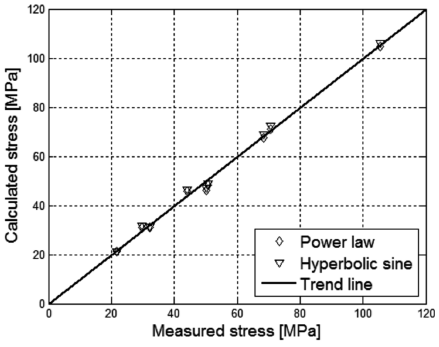

Fig. 4. Steel 1 calculated-measured stress.

3.2. Microstructure

TEM analysis revealed fully martensitic microstructure in all deformed specimens. Very similar microstructure was found after quenching, independently of deformation temperature and rates; this is probably related to the very high intrinsic hardenability of both steels: in these materials, the austenite grain size effect on hardenability is negligible, so that also the effect of hot deformation on it is hidden by intrinsic hardenability mainly due to the Cr effect. In Fig. 5 microstructure as obtained by TEM is reported for steel 1 in two deformation conditions ($T/\dot{\varepsilon} = 1000\,^{\circ}\mathrm{C}/0.01$ s^{-1}, $T/\dot{\varepsilon} = 1200\,^{\circ}\mathrm{C}/1.00$ s^{-1}).

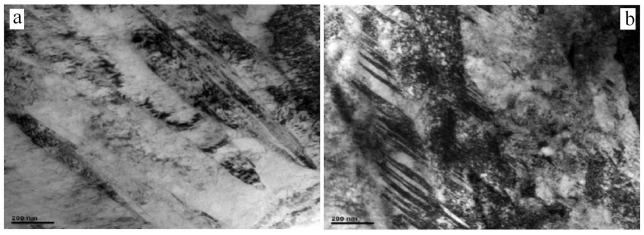

Fig. 5. Microstructure by TEM of the steel 1: (a) $T/\dot{\varepsilon} = 1000\,^{\circ}\mathrm{C}/0.01$ s^{-1}, (b) $T/\dot{\varepsilon} = 1200\,^{\circ}\mathrm{C}/1.00$ s^{-1}.

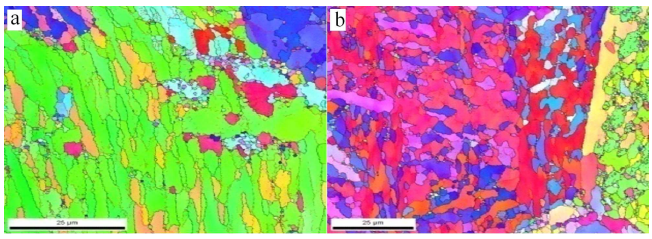

Fig. 6. Microstructure by EBSD in steel 1: (a) $T/\dot{\varepsilon} = 1000\,^{\circ}\mathrm{C}/0.01$ s^{-1}, (b) $T/\dot{\varepsilon} = 1200\,^{\circ}\mathrm{C}/1.00$ s^{-1}.

EBSD analysis of the same specimens (Fig. 6) shows a very fine microstructure, independent of austenite grain size (deformation temperature), as expected for martensite [9]. Since is it not possible to evaluate the recrystallization degree of austenite, it is reasonably assumed that recrystallized austenite leads to a low (< 1) GOS parameter in martensite after quenching. Figures 7 and 8 show a higher volume martensite fraction with GOS < 1 if deformation temperatures or rates are increased.

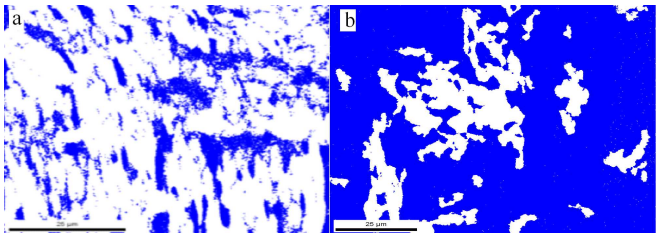

Fig. 7. GOS maps by EBSD in steel 1: (a) $T/\dot{\varepsilon} = 1000\,^{\circ}\mathrm{C}/0.01$ s^{-1}, (b) $T/\dot{\varepsilon} = 1200\,^{\circ}\mathrm{C}/1.00$ s^{-1}. Blue code: GOS < 1, white code: GOS > 1.

4. Conclusions

The hot deformation of a 3% Cr and a 5% Cr steels was investigated by means of torsion tests in a wide range of temperature and strain rate. Both steels showed a dynamic recrystallization behavior during hot deformation. The hot deformability of the two steels appeared to be very similar: in particular in both cases a higher martensite volume fraction characterized by grain orientation spread GOS < 1 was found with increasing deformation temperatures or rates. The recrystallization volume appeared to be dependent of the degree of austenite recrystallization.

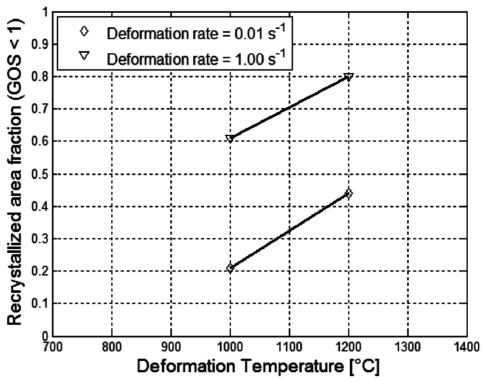

Fig. 8. Steel 1 recrystallized volume fraction as a function of deformation temperatures and deformation rates.

References

[1] H.J. McQueen, E. Evangelista, in: *Proc. 2nd Int. Conf. on Superhigh Strength Steels, Milano (Italy)*, 2010.

[2] E. Evangelista, M. Masini, M. El Methedi, S. Spigarelli, *J. Alloys Comp.* **378**, 151 (2004).

[3] H.J. McQueen, J.J. Jonas, *Metal Forming: Interrelation between Theory and Practice*, Plenum Press, New York 1971.

[4] T. Sakai, A. Belyakov, R. Kuibyshev, H. Miura, J.J. Jonas, *Prog. Mater. Sci.* **60**, 130 (2014).

[5] C. Imbert, N.D. Ryan, H.J. McQueen, *Metall. Mater. Trans. A* **15**, 1855 (1984).

[6] C. Imbert, H.J. McQueen, *Mater. Sci. Tech. Ser.* **16**, 532 (2000).

[7] H.J. McQueen, A.C. Imbert, in: *Proc. Int. Conf. Thermomechanical Processing and Mechanical Properties of Hypereutectoid Steels, Warrendale*, 1997, TMS-AIME, p. 55.

[8] H.J. McQueen, E. Evangelista, N. Ryan, in: *Proc. Int. Conf. on Thermomechanical Processing: Mechanics, Microstructure and Control, Sheffield*, 2003, p. 359.

[9] M.F. Abbod, C.M. Sellars, A. Tanaka, D.A. Linkens, M. Mahfouf, *Mater. Sci. Eng. A* **491**, 290 (2008).

[10] A. Di Schino, L. Alleva, M. Guagnelli, *Mater. Sci. Forum* **715-716**, 860 (2012).

[11] Y. Jin, M. Bernacki, G.S. Rohrer, A.D. Rollett, B. Lin, N. Bozzolo, *Mater. Sci. Forum* **113–116**, 120 (2013).

[12] L. Lianos, B. Pereda, D. Jorge-Badiola, J.M. Rodriguez-Ibabe, B. Lopez, *Mater. Sci. Forum* **753**, 443 (2013).